Autistic traits, but not schizotypy, predict overweighting of sensory information in Bayesian visual integration : Supplementary Material

P. Karvelis, A. R Seitz. S. Lawrie and P. Seriès

November 3, 2017

1 Supplementary Figures

In order to ensure that participants performed adequately in the psychophysical task, we used a predetermined performance criteria for inclusion into the study. Firstly, participants were required to detect the motion stimuli on more than 80% of trials with the high contrast motion stimuli and also make active estimates of the motion directions by clicking the mouse. Secondly, their average estimation performance on the high contrast stimuli had to be within 30° of the correct angle. 8 out of 91 participants failed to satisfy at least one of the criteria: 2 participants did not satisfy the first criteria, 4 did not satisfy the second criteria and 2 did not satisfy both of the criteria (Supplementary Figure 1). These participants were excluded from further analysis.

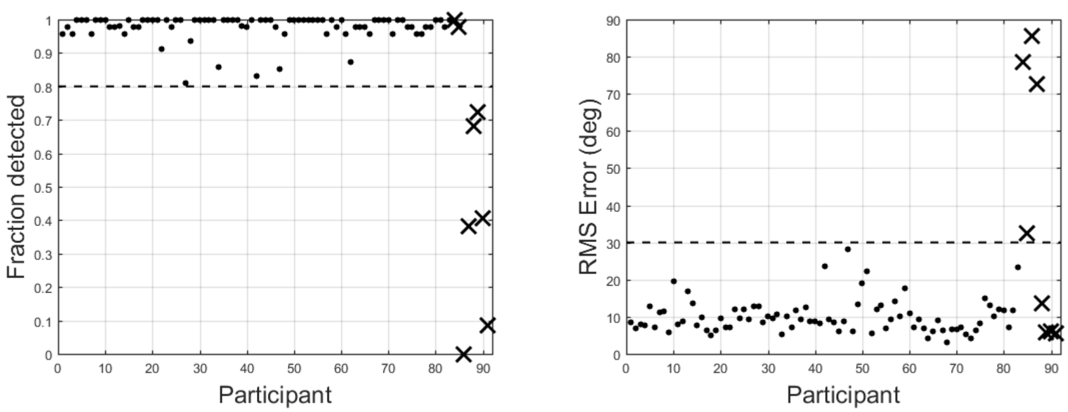

Figure 1: Task performance at the highest contrast level and exclusion Criteria. **Left panel**: fraction of detected high contrast trials - quantified as the fraction of trials in which participants both validated their choice with a click within 3000 ms in the estimation part and reported seeing dots (clicked "DOTS") in the detection part. **Right panel**: root mean square error of estimations on high contrast trials. The dashed lines represent minimum performance criteria (more than 80% detection and less than 30° RMS error of estimations). Excluded participants are denoted by cross markers.

Supplementary Figure 2 describes the average convergence of the contrast staircases. Two groups comprising our sample performed the task at different background contrast levels. For a subgroup of 50 participants (left panel), the background luminance was set to 1.16 cd/m2 for the other sub-group of 41 (right panel) it was set to 5.18 cd/m2. For both groups, contrast staircases converged after 170 trials for both intermediate contrast levels, denoted with the vertical dashed line. In both groups, 2/1 and 4/1 staircased contrasts were considerably overlapping: on average 2/1 being 0.20±0.04 cd/m^2 and 4/1 being 0.22±0.04 cd/m^2 above the 1.16 cd/m^2 background luminance; and on average 2/1 being 0.42±0.05 cd/m^2 and 4/1 being 0.46±0.05 cd/m^2 above the 5.18 cd/m^2 background luminance. Thus, the two intermediate contrasts were combined for all further data analysis.

Supplementary Figure 3 shows the correlations between schizotypy scores and task performance. There were no significant correlations with any of the measures.

Supplementary Figure 4 shows a representative sample of the priors we extracted for a number of individuals, using the 'BAYES' model.

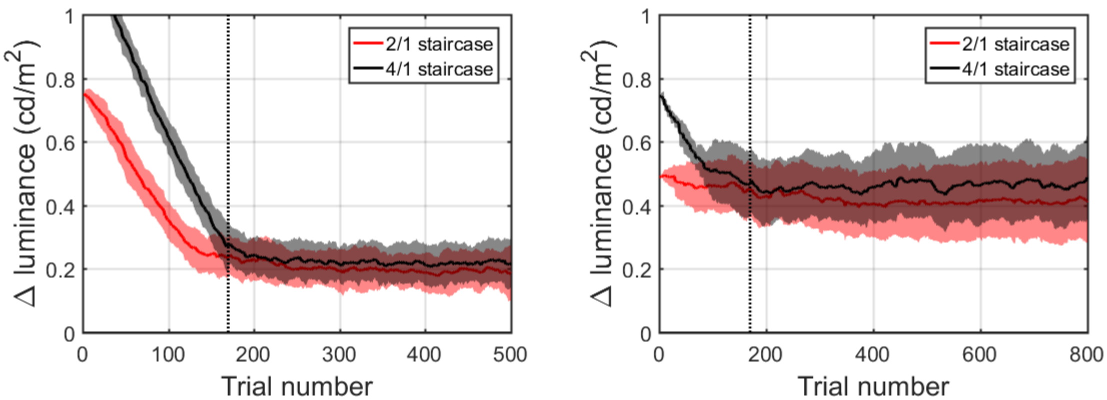

Figure 2: Population averaged stimulus contrast relative to the background contrast for the 2/1 (red) and 4/1 (black) staircased contrast levels. Standard deviation is denoted by shaded areas with corresponding colors. The vertical dashed line marks 170 trials. **Left panel**: 44 participants (remaining after exclusion) that performed the task with the background luminance set to 1.16 cd/m^2. **Right panel**: 39 participants (remaining after exclusion) that performed the task with the background luminance set to 5.18 cd/m^2.

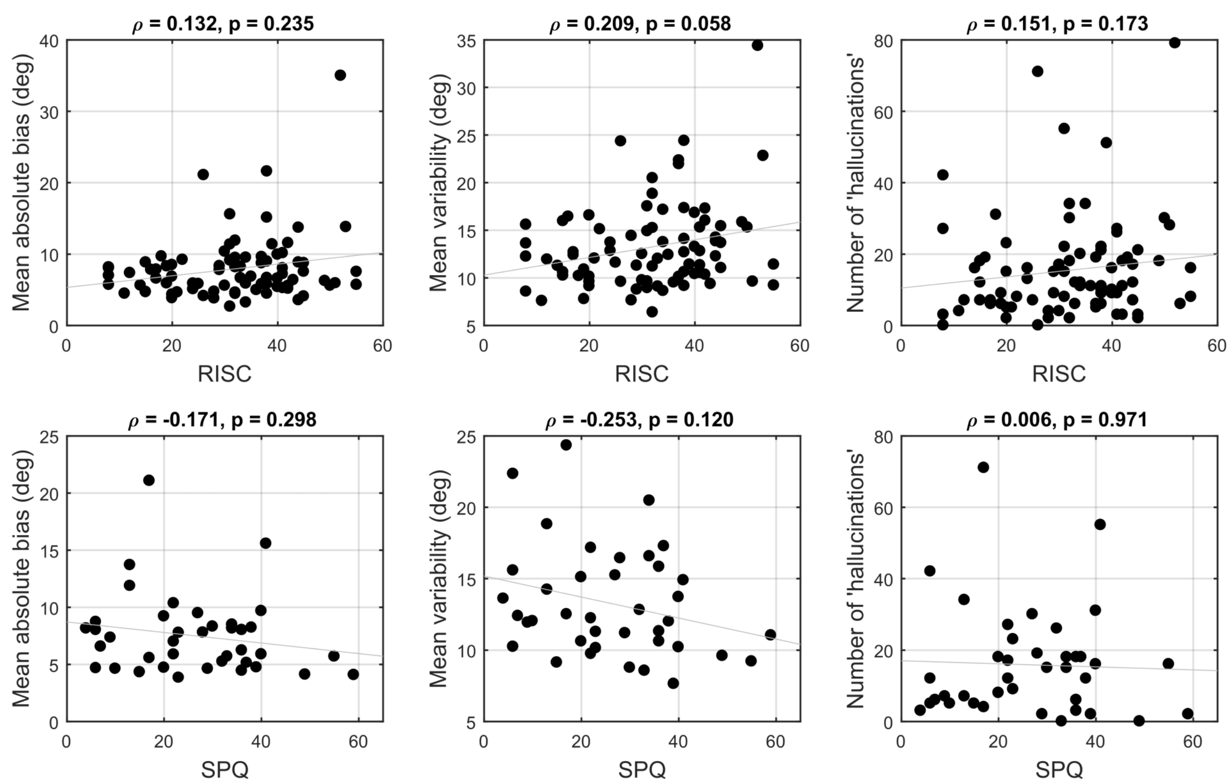

Figure 3: Correlations between personality traits, RISC (**top row**) and SPQ (**bottom row**) and task performance. There were no significant correlations with any of the measures: mean absolute bias (**left column**), mean estimation variability (**middle column**) and total number of 'hallucinations' (**right column**). Spearman's coefficients and p-values are indicated above each plot.

Supplementary Figure 5 describes the correlations between the BAYES model parameter values and schizotypy scores. There was no significant correlation with any of the parameters.

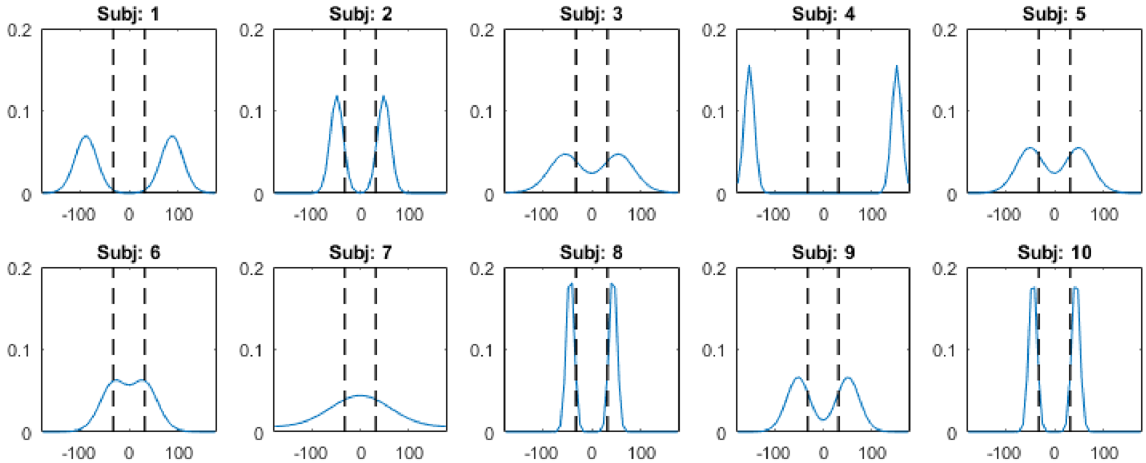

Figure 4: A representative sample of prior expectations for each individual as reconstructed via 'BAYES' model. The dashed lines correspond to the two most frequently presented motion directions (±32°).

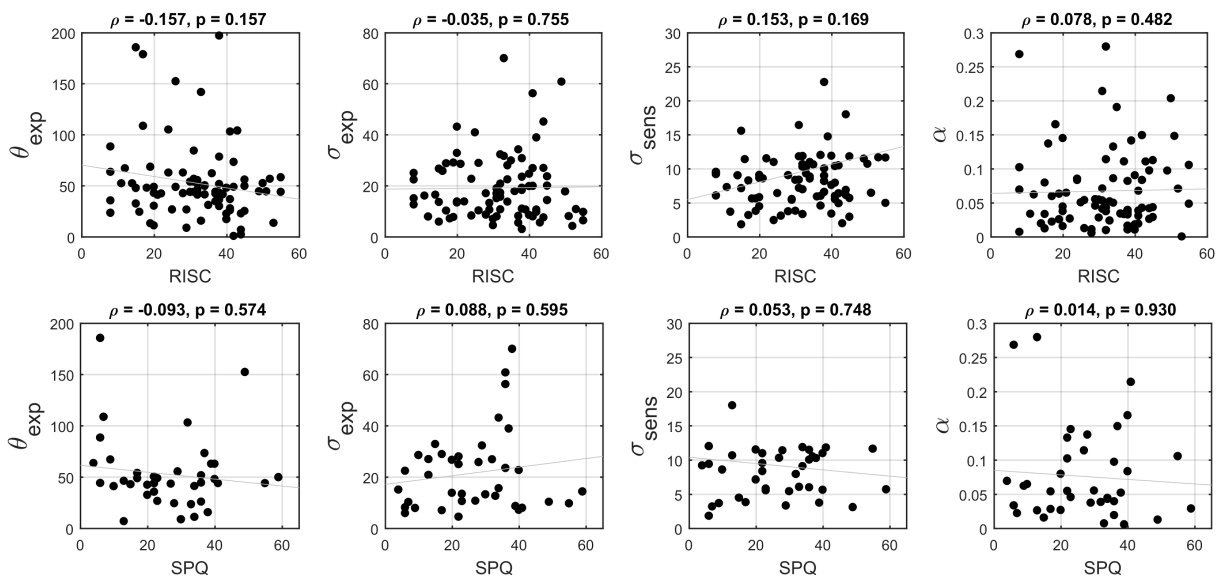

Figure 5: Correlations with the BAYES model parameter values and schizotypy traits (as measured by both RISC and SPQ). **First column**: θ_{exp} - mean of the prior expectations, **second column**: σ_{exp} - uncertainty of the prior distribution, **third column**: σ_{sens} - uncertainty in the sensory likelihood and **fourth column**: α - fraction of random estimations. Spearman's coefficients and p-values are indicated above each plot.

2 Combining the different background luminance levels

To compare the two sub-groups that performed the task at different background luminance levels, we performed Wilcoxon two-tailed rank sum test for all of the behavioral measures and none of them indicated any differences: mean absolute estimation bias (z = 0.652; ranksum = 1920; p = 0.514), mean variance of estimations (z = -0.406; ranksum = 1803; p = 0.685), total number of hallucinations (z = 0.128; ranksum = 1862; p = 0.898) number of hallucinations within 8° of ±32° (z = 0.870; ranksum = 1943; p = 0.384), mean estimation reaction time (z = 0.479; ranksum = 1901; p = 0.632). The two groups were therefore combined.

3 Temporal emergence of the impact of expectations

We investigated how many trials it took for the acquired prior effects to impact behavior. First, we looked at estimation reaction times (RT) and compared mean RT of each individual at $\pm 32°$ with mean RT at all other directions; we compared cumulative moving averages at every 30 trials (**Supplementary Fig. 6**). We found that it took less than 150 trials for RT at $\pm 32°$ to become significantly shorter than average RT at all other directions (**Supplementary Fig. 6** and p-values within).

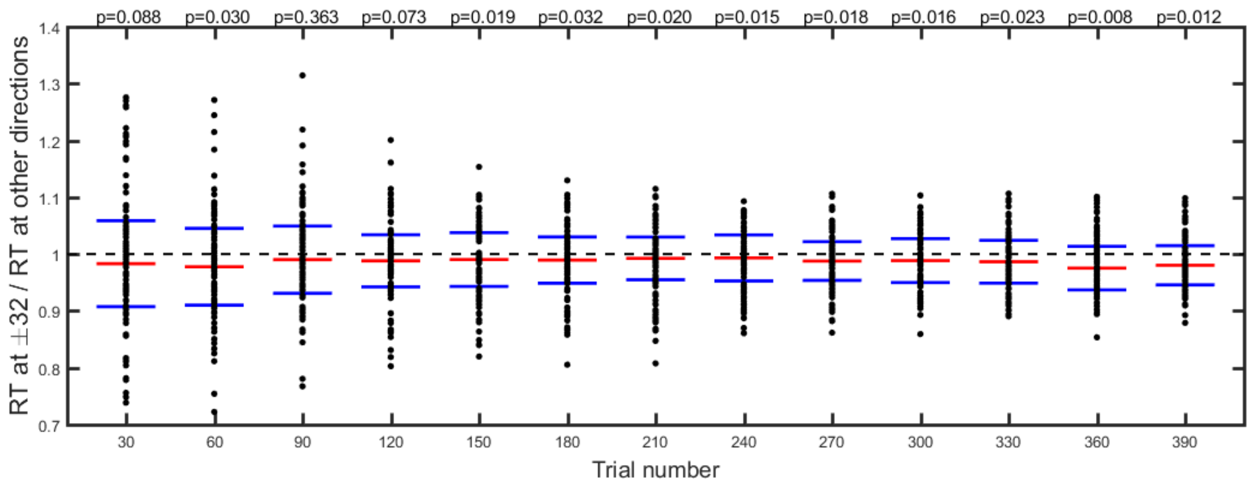

Figure 6: Cumulative moving average of ratio of estimation reaction times at $\pm 32°$ vs average reaction times at all other directions. Red bars indicate median values and blue bars indicate 25th and 75th percentiles. p-values indicate whether RTs at $\pm 32°$ are significantly shorter than average RTs over all other directions (one-tailed Wilcoxon signed rank test).

Similarly, we looked at average detection performance and compared the fraction of trials in which stimulus was detected at $\pm 32°$ with the mean fraction detected over all other presented directions; again, we compared cumulative moving averages at every 30 trials (**Supplementary Fig. 7**). We found that it took less than 120 trials for detection at $\pm 32°$ to become significantly better than average detection over all other presented directions (**Supplementary Fig. 7** and p-values within).

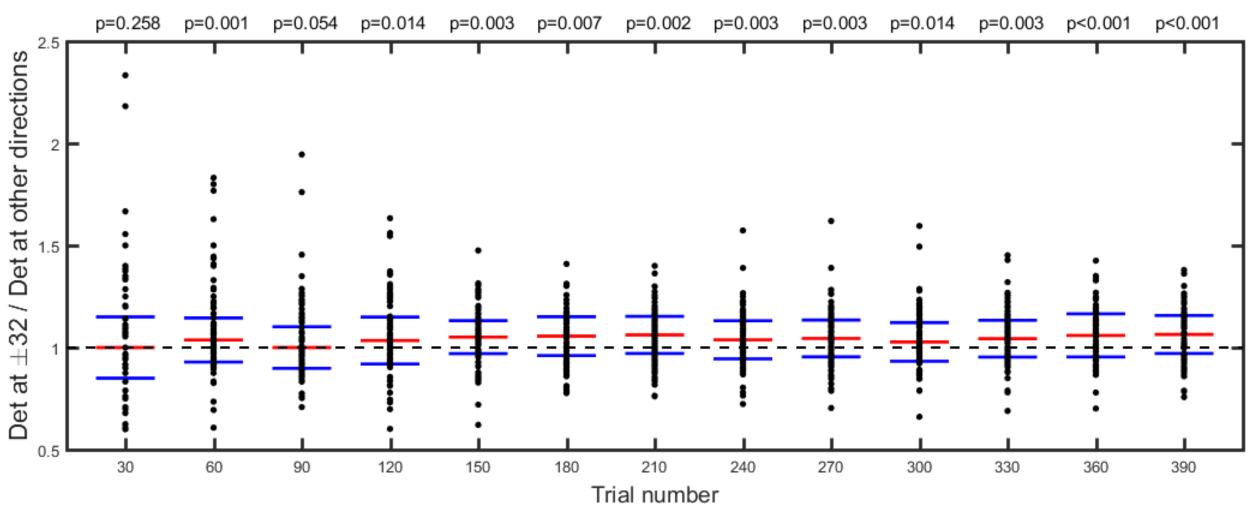

Figure 7: Cumulative moving average of ratio of fraction of detected stimuli at $\pm 32°$ vs average fraction detected at all other directions. Red bars indicate median values and blue bars indicate 25th and 75th percentiles. p-values indicate whether fraction detected at $\pm 32°$ are significantly larger than average fraction detected over all other directions (one-tailed Wilcoxon signed rank test).

Lastly, for trials where no stimulus was presented, we looked at how long it took participants to start 'hallucinating' predominantly around ±32° as opposed to all other possible directions. This was quantified as a probability ratio p_{rel}:

$$p_{rel} = p(\theta_{est} = \pm 32(\pm 8)^{\circ}) \cdot N_{bins} \ , \tag{1}$$

where N_{bins} is the number of bins (45), each of size 16°. This probability ratio would be equal to 1 if participants were equally likely to estimate within 8° of ±32° as they were to estimate within other bins. Again, we computed cumulative moving mean at every 30 trials (**Supplementary Fig. 8**). For participants who did not report seeing dots at any direction within a given number of trials (i.e. zero total 'hallucinations') this probability ratio was undefined, therefore, those individuals were omitted from significance test at that point. We found that it took less than 210 trials for p_{rel} to become significantly larger than 1 (**Supplementary Fig. 8** and p-values within).

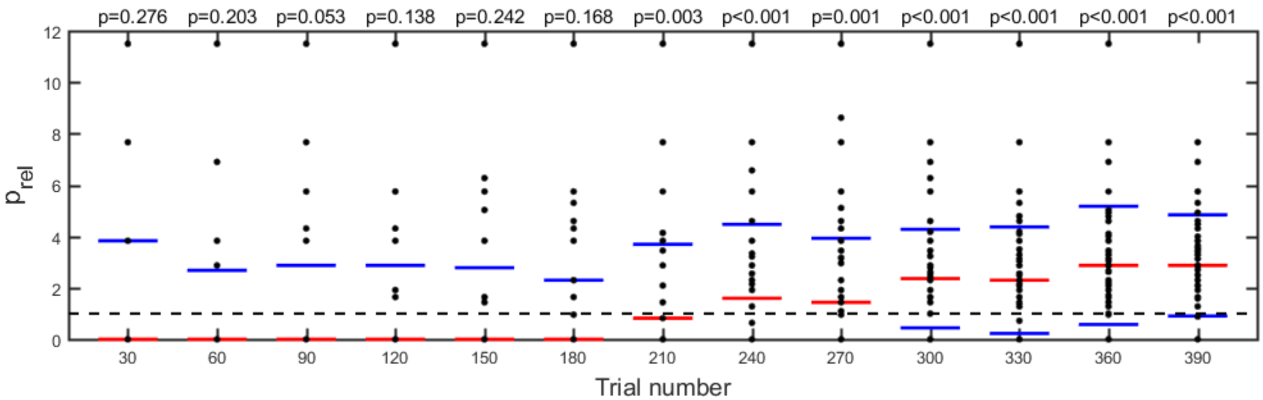

Figure 8: Cumulative moving average of ratio of fraction of detected stimuli at ±32° vs average fraction detected at all other directions. Red bars indicate median values and blue bars indicate 25th and 75th percentiles. p-values indicate whether fraction detected at ±32° are significantly larger than average fraction detected over all other directions (one-tailed Wilcoxon signed rank test).

4 Non-symmetric prior models

The stimulus distribution is multimodal and symmetric. Learning such a distribution might be inherently difficult. We reasoned that some individual differences might lie in asymmetries of the acquired priors. Therefore, we explored an alternative parameterization of the acquired priors which allowed them to be asymmtrical. We allowed the two modes in the prior to have different position with respect to 0° and to have different amount of probability associated with each mode. This resulted in:

$$p_{exp}(\theta) = (1 - \pi) \cdot V(\theta_p, \kappa_p) + \pi \cdot V(\theta_n, \kappa_p) \quad , \tag{2}$$

where π ($\in$ [0 1]) is a mixing parameter. Using this parameterization we fitted 'BAYES' model as described in the main text (thus, we denoted this alternative model as 'BAYES_π'). The alternative parameterization did not result in a better BIC as compared to 'BAYES' model (p = 0.378, signed rank test). In addition, we performed parameter recovery to determine how robust 'BAYES_π' is and found that recovering the mixing parameter π was not very reliable (r=0.4), although other parameters retained their previous reliability (**Fig. 9**). We thus focussed on the simpler model in the current study.

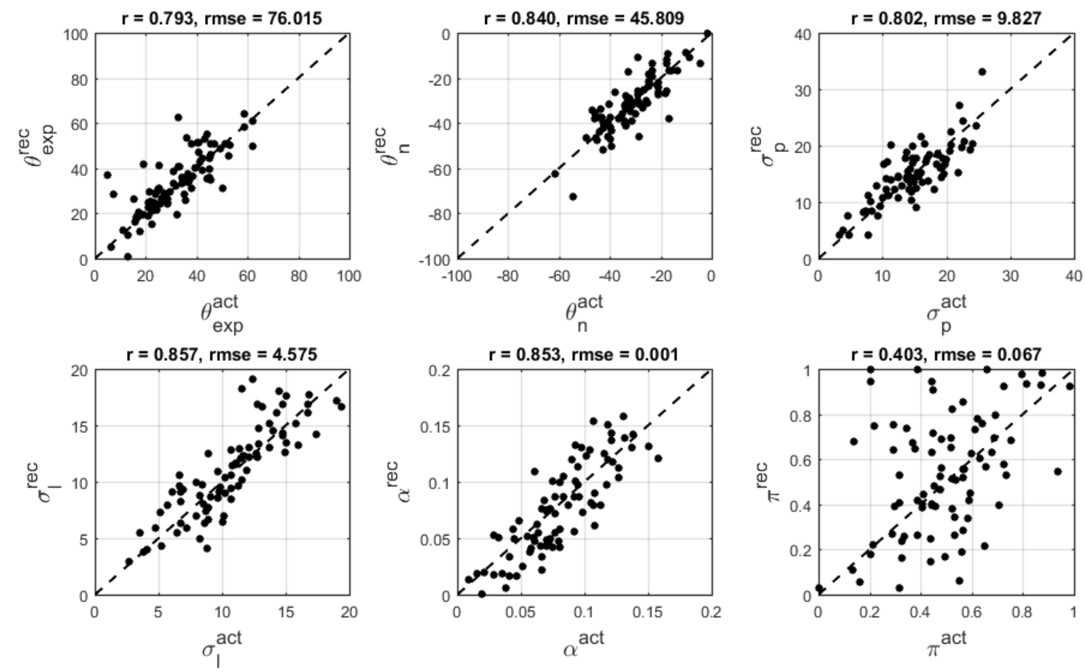

Figure 9: Comparison of actual and recovered parameters via 'BAYES_π' model. θ_{exp} and θ_n - positive and negative modes of the bimodal distribution of prior expectations, σ_p - uncertainty of the prior distribution, σ_l - uncertainty in the sensory likelihood, α - fraction of random estimations, π - mixing parameter responsible for the degree of bimodality. Actual parameters are scattered along x-axis and recovered parameters are scattered along y-axis. The dashed diagonal line is a reference line indicating perfect parameter recovery. Pearson's correlation coefficients are indicated above each plot.

5 Response bias models

We wanted to account for the possibility that the task behavior might be better explained by simple behavioral strategies. This class of models assumed that on trials when participants were unsure about the presented motion direction they made an estimation based solely on prior expectations, while on the remaining fraction of trials they made unbiased estimates based solely on sensory input.

5.1 ADD1

The first model ('ADD1') assumed that when participants were unsure about which motion direction they had perceived, they made an estimate that was close to one of the two most frequently presented motion directions.

In this model, on each trial, participants make a sensory observation of the stimulus motion direction, θ_{obs}.

We parameterize the probability of observing the stimulus to be moving in a direction θ_{obs} by a von Mises (circular normal) distribution centered on the actual stimulus direction and with width determined by $1/k_l$:

$$p_{sens}(\theta_{sens}|\theta_{act}) = V(\theta_{act}, k_{sens}) \tag{3}$$

.

On most trials, we assume that participants make a perceptual estimate of the stimulus motion direction (θ_{perc}) that is based entirely on their sensory observation so that $\theta_{perc} = \theta_{obs}$.

However, on a certain proportion of trials, when participants are uncertain about whether a stimulus was present or not, they resort to their "expectations" by making a perceptual estimate that is sampled from a learned distribution, $p_{exp}(\theta)$.

For simplicity, we parameterize this distribution as the sum of two circular normal distributions, each with width determined by $1/k_{exp}$, and centered on motion directions $-\theta_{exp}$ and θ_{exp}, respectively.

Finally, we accommodate for the fact that there will be a certain amount of noise associated with moving the estimation bar to indicate which direction the stimulus is moving in as well as allowing for a fraction of trials α, where participants make estimates that are completely random. Thus, the estimation response θ_{est} is related to the perceptual estimate θ_{perc} via the equation:

$$p(\theta_{est}|\theta_{perc}) = (1{-}\alpha){\cdot}V(\theta_{perc}, k_m) + \alpha. \tag{4}$$

Bringing all this together, the distribution of estimation responses for a single participant is given by:

$$p(\theta_{est}|\theta_{act}) = (1{-}\alpha)[(1\text{-a}(\theta))p_l(\theta_{obs} = \theta_{est}|\theta_{act}) + a(\theta)p_{exp}(\theta_{est})] * V(0, k_m) + \alpha. \tag{5}$$

where the asterisk denotes a convolution and $a(\theta)$ determines the proportion of trials that participants sampled from the "expected" distribution, $p_{exp}(\theta)$.

The resulting 'ADD1' model has 9 free parameters θ_{exp}, k_{exp}, $a(\theta)$ (which can take a different value for each of the 5 angles: 0, ±16, ±32, ±48, ±64), k_{sens} and α.

5.2 ADD2

The second model, 'ADD2', was just as 'ADD1' except that it had slightly more complex strategy for trials when participants were unsure about the stimulus motion direction: instead of sampling from the complete learned probability distribution ranging from $-180°$ to $+180°$ (Eq. (11)), they effectively truncated this distribution on a trial by trial basis and sampled from only one part of it, negative (-180 to $0°$) or positive (0 to $+180°$), depending on which side of the distribution the actual stimulus occurred.

Incorporating this into the distribution of estimation responses gives:

$$p(\theta_{est}|\theta_{act}) = (1{-}\alpha)[(1\text{-a}(\theta)\text{-b}(\theta))p_l(\theta_{obs} = \theta_{est}|\theta_{act}) + a(\theta)p_{expN}(\theta_{est}) + b(\theta)p_{expP}(\theta_{est})] * V(0, k_m) + \alpha. \tag{6}$$

where asterisk ($*$) denotes convolution; a(ϑ) and b(ϑ) determine the proportion of trials in which participants sample from either anticlockwise or clockwise distributions $p_{expN}(\theta)$ and $p_{expP}(\theta)$, respectively.

In addition, we also considered slight variations of the 'ADD1' and 'ADD2' models, denoted 'ADD1_m' and 'ADD2_m' respectively. These were identical to 'ADD1' and 'ADD2' except from setting $1/k_{exp}$ to zero; that is, on trials when perceptual estimates were derived only from expectations, they were equal to the mode of the learnt distribution (i.e. no uncertainty).

6 Full models (estimation + detection)

We have built a Bayesian model that incorporates both estimation and detection performance ('BAYES_full') in order to fully account for the task behavior. This time, the acquired priors consisted of both the expectations about the direction of stimuli motion (θ) and the expectations about whether stimulus is presented (s=1) or not (s=0). It was parameterized as:

$$p_{exp}(\theta, s) = \begin{cases} (1-b) \cdot \frac{1}{2\pi}, & \text{if } s = 0 \\ b \cdot \frac{1}{2}[V(-\theta_{exp}, \kappa_{exp}) + V(\theta_{exp}, \kappa_{exp})], & \text{if } s = 1 \end{cases}$$

where parameter b accounts for a participant's average expectation that the stimulus will be presented. Thus, we assumed that expectations about motion direction were uniform for when no stimulus was expected. While the expectations about motion direction when the stimulus was expected followed the bimodal probability distribution just as in the previous models.

On each trial, given the presented motion direction (θ_{act}) and the presence of the stimulus (s), participants made sensory measurements $p_{sens}(\theta_{sens}, s_{sens}|\theta_{act}, s)$. For simplicity, we assumed that the sensory probability of whether the stimulus was present ($p_{sens}(s_{sens}|\theta_{act}, s)$) was independent of the sensory input about the motion direction ($p_{sens}(\theta_{sens}|\theta_{act}, s)$). We further assumed that s_{sens} was independent of the presented motion direction θ_{act}, as informed by 'BAYES_var' model (that allowed the sensory likelihood to vary based on the presented motion direction), which did not produce a better fit. As before, the mean of the motion direction was allowed to fluctuate on trial-by-trial basis, such that:

$$p(\theta|\theta_{act}) = V(\theta_{act}, \kappa_{sens}) \quad , \tag{7}$$

where $1/\kappa_{sens}$ is sensory noise. Given the estimate of the mean θ, the sensory input θ_{sens} is represented with the associated uncertainty via:

$$p_{sens}(\theta_{sens}|\theta) = V(\theta, \kappa_{sens}) \quad . \tag{8}$$

Putting all this together, the sensory likelihood was expressed as:

$$p_{sens}(\theta_{sens}, s_{sens}|\theta, s) = p_{sens}(\theta_{sens}|\theta, s)p(s_{sens}|s) \quad , \tag{9}$$

where $p_{sens}(\theta_{sens}|\theta_{act}, s)$ was parameterized as:

$$p_{sens}(\theta_{sens}|\theta_{act}, s) = \begin{cases} \frac{1}{2\pi}, & \text{if } s = 0 \\ V(\theta, \kappa_{sens}), & \text{if } s = 1 \end{cases}$$

where we assumed that sensory likelihood is uniform when no stimulus is presented. Finally, $p_{sens}(s_{sens}|s)$ was parameterized as:

$$p_{sens}(s_{sens} = \{0, 1\}|s) = \begin{cases} \{1-c, c\}, & \text{if } s = 0 \\ \{1-d, d\}, & \text{if } s = 1 \end{cases}$$

where parameter c is the average probability of detecting dots when they are not presented, and parameter 'd' is the average probability of detecting dots when they are presented. Putting together prior and likelihood, the resulting posterior probability distribution becomes:

$$p_{post}(\theta, s|\theta_{sens}, s_{sens}) \propto p_{sens}(\theta_{sens}|\theta, s) \cdot p_{sens}(s_{sens}|s) \cdot p_{exp}(\theta, s) \quad , \tag{10}$$

With a given posterior participants could have performed detection task at least in two ways. One way is to maximize the posterior (i.e. to always choose the value of s that has higher probability):

$$s_{perc} = \underset{s}{\operatorname{argmax}}[p_{post}(s|\theta_{sens}, s_{sens})] \tag{11}$$

Another way is to perform probability matching and choose in accordance to the size of the probabilities:

$$s_{perc} = \begin{cases} 0 \ , & \text{if } p_{post}(s = 0|\theta_{sens}, s_{sens}) > \eta \\ 1 \ , & \text{if } p_{post}(s = 0|\theta_{sens}, s_{sens}) < \eta \end{cases}$$

where $\eta \in [0\ 1]$ and is drawn for each trial from a uniform distribution. We considered both of these possibilities and implemented a variant of the model for each.

Finally, just as in 'BAYES' model, the motion direction percept was formed by taking the mean of the posterior:

$$\theta_{perc} = \int \theta \cdot p_{post}(\theta|\theta_{sens}, s_{sens})\ d\theta\ = \frac{1}{Z} \int \theta \cdot \sum_{s} p_{exp}(\theta) \cdot p_{sens}(\theta_{sens}|\theta, s) \cdot p_{sens}(s_{sens}|s)\ d\theta\ , \quad (12)$$

As previously, we accounted for motor noise and the lapse responses via:

$$p(\theta_{est}|\theta_{perc}) = (1-\alpha) \cdot V(\theta_{perc}, \kappa_{motor}) + \alpha \cdot p_{exp}(\theta) * V(0, \kappa_{motor})\ . \quad (13)$$

In total, 'BAYES_full' model had 7 free parameters. To fit the model, in addition to intermediate contrast trials, we also used no-stimulus trial data. The rest of the fitting procedure was the same as in the main text: we built a distribution of 1,000 posterior estimations for each presented angle and one more distribution of 1,000 posterior estimations for no stimulus trials.

We found that 'BAYES_full' provided a good fit and captured the main features of both estimation and detection performance (**Supplementary Fig. 10**). As before, to test how reliable parameters estimated for 'BAYES_full' model are, we performed parameter recovery. Just as for 'BAYES' parameter recovery described in the main text, we generated 80 sets of parameters and simulated 200 trials of data with 'BAYES_full' model for each of them. Then we fitted 'BAYES_full' to the simulated data. The results revealed that parameters 'd' and 'c' had very poor recovery (**Supplementary Fig. 11**). We thus focussed on the simpler model in the current study.

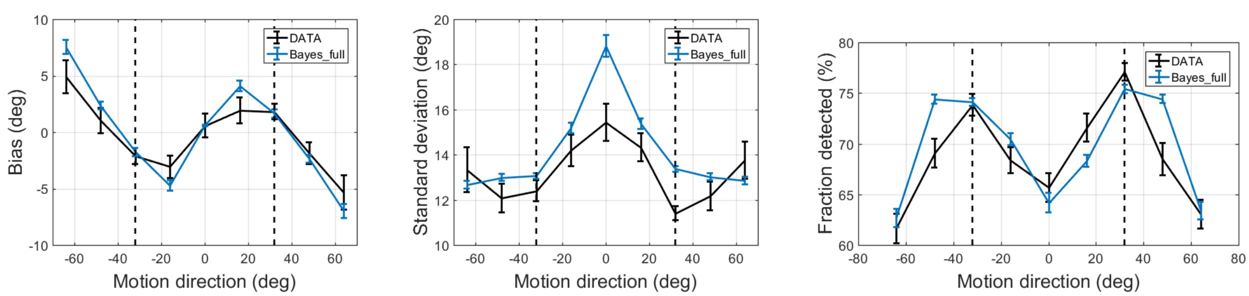

Figure 10: Task performance as predicted by the BAYES_full model. **Left panel:** mean estimation bias at different motion directions. **Middle panel:** standard deviation of estimations at different motion directions. **Right panel:** fraction of detected stimuli at different motion directions. The dashed lines correspond to the two most frequently presented motion directions (±32°). Error bars represent within-subject standard error.

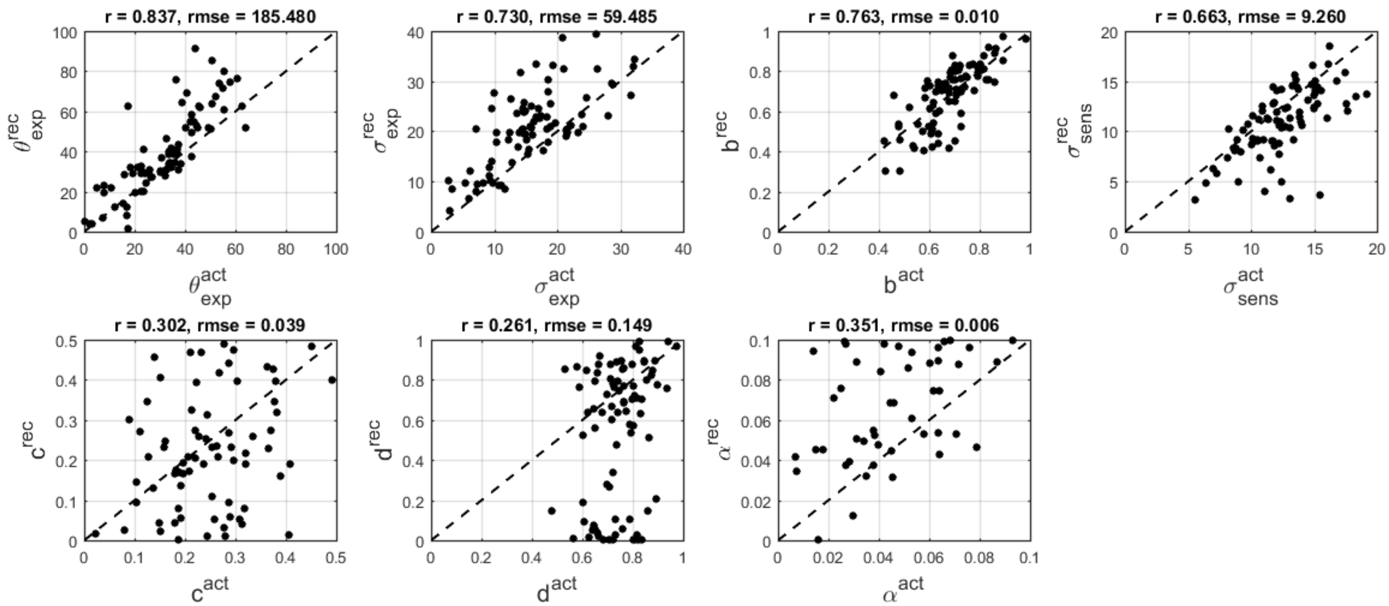

Figure 11: Comparison of actual and recovered parameters via 'BAYES_full' model. θ_{exp} - the mean of prior expectations of motion direction, σ_{exp} - uncertainty of the prior expectations of motion direction, σ_{sens} - uncertainty in the sensory likelihood, α - fraction of random estimations, b - prior expectation for dots being presented, c - likelihood of detecting the dots when they are not presented, d - likelihood of detecting the dots when they are presented. Actual parameters are scattered along x-axis and recovered parameters are scattered along y-axis. The dashed diagonal line is a reference line indicating perfect parameter recovery.